Computers and Mathematics with Applications 64 (2012) 2695–2711

Contents lists available at SciVerse ScienceDirect

Computers and Mathematics with Applications

journal homepage: www.elsevier.com/locate/camwa

Boundary element formulations for the numerical solution of two-dimensional diffusion problems with variable coefficients

M.A. AL-Jawary [a], J. Ravnik [b], L.C. Wrobel [a,*], L. Škerget [b]

[a] School of Engineering and Design, Brunel University, Uxbridge UB8 3PH, UK

[b] Faculty of Mechanical Engineering, University of Maribor, Smetanova 17, SI-2000 Maribor, Slovenia

ARTICLE INFO

Article history:
Received 16 March 2012
Received in revised form 12 June 2012
Accepted 7 August 2012

Keywords:
Boundary element method
Variable coefficient
Boundary–domain integral equation
Boundary–domain integro-differential equation
Radial integration method
Domain decomposition

ABSTRACT

This paper presents new formulations of the radial integration boundary integral equation (RIBIE) and the radial integration boundary integro-differential equation (RIBIDE) methods for the numerical solution of two-dimensional diffusion problems with variable coefficients. The methods use either a specially constructed parametrix (Levi function) or the standard fundamental solution for the Laplace equation to reduce the boundary-value problem (BVP) to a boundary–domain integral equation (BDIE) or boundary–domain integro-differential equation (BDIDE). The radial integration method (RIM) is then employed to convert the domain integrals arising in both BDIE and BDIDE methods into equivalent boundary integrals. The resulting formulations lead to pure boundary integral and integro-differential equations with no domain integrals. Furthermore, a subdomain decomposition technique (SDBDIE) is proposed, which leads to a sparse system of linear equations, thus avoiding the need to calculate a large number of domain integrals. Numerical examples are presented for several simple problems, for which exact solutions are available, to demonstrate the efficiency of the proposed approaches.

1. Introduction

The boundary element method (BEM) has become an efficient and popular alternative to the finite element method (FEM) because of its ability, at least for some problems with constant coefficients, to reduce a BVP for a linear partial differential equation (PDE) defined in a domain to an integral equation defined on the boundary, leading to a simplified discretization process with boundary elements only. The main requirement for the reduction of the PDE to a boundary integral equation (BIE) is that a fundamental solution to the PDE must be available. Such fundamental solutions are well known for many PDEs with constant coefficients (see [1–4]), but are not generally available when the coefficients of the original PDE are variable.

BEM formulations for solving nonlinear, non-homogeneous problems and problems with variable coefficients usually adopt fundamental solutions for a simplified linear, homogeneous problem with constant coefficients, generating domain integrals in the corresponding integral equation. This feature makes the BEM less attractive, as a domain discretization is then required.

Several methodologies have been proposed in order to overcome these difficulties. One possible technique is to find a fundamental solution for the nonlinear, non-homogeneous problem or a problem with variable coefficients which can provide a pure boundary integral equation. Unfortunately, these fundamental solutions are only available for some very special cases [5–8]. A methodology was developed by Kassab and Divo [9] in which generalized fundamental solutions are

* Corresponding author.
E-mail addresses: Majeed.AL-Jawary@brunel.ac.uk (M.A. AL-Jawary), jure.ravnik@uni-mb.si (J. Ravnik), Luiz.Wrobel@brunel.ac.uk (L.C. Wrobel), leo@uni-mb.si (L. Škerget).

0898-1221/$ – see front matter © 2012 Elsevier Ltd. All rights reserved.
doi:10.1016/j.camwa.2012.08.002

used to achieve boundary integral equations for heat conduction problems with spatially varying conductivity. Kassab and Divo's technique is based on developing a generalized forcing function rather than using the Dirac delta function in the derivation of the fundamental solutions. This technique can solve many problems, although issues have been raised by some researchers [10,11]. In addition, as this technique has been developed for homogeneous problems, a domain integral will still appear when dealing with heat sources.

An alternative methodology for solving PDEs with variable coefficients with the BEM without domain discretization involves the transformation of the domain integrals appearing in the integral equation, derived by using fundamental solutions for linear homogeneous problems, into equivalent boundary integrals. There are two powerful techniques available in the literature. The first is the dual reciprocity method (DRM) developed by Nardini and Brebbia [12]. In this method, the transformation is carried out by approximating the source term with a series of basis functions and by using their particular solutions. A detailed description and practical applications of this method can be found in the book of Partridge et al. [13]. The drawback of this technique is that the particular solutions may be difficult to obtain for some complicated problems, depending on the radial basis function (RBF) adopted. In addition, even for known source terms, the method still requires an approximation of the known function using RBFs [14].

More recently, a new transformation technique, the RIM, has been developed by Gao [14,15]. The RIM can transform any complicated domain integral to the boundary, while also removing various singularities appearing in the domain integrals. The main feature of the RIM is that it can treat different kinds of domain integrals in a unified way since it does not resort to particular solutions as in the DRM.

The RIM was implemented in [15] for the analysis of elastoplastic problems, in which case strong and weak singularities were removed by transforming the domain integrals to the boundary. The RIM was also applied to thermoelastic problems in [16], in which case the domain integrals included in both displacement and internal stress integral equations were transformed into equivalent boundary integrals. The Green's function for Laplace's equation was used to derive a boundary–domain integral equation for heat conduction problems with heat generation and spatially varying conductivity in [17]. Then, the RIM was adopted to convert the domain integrals for both heat generation and variable thermal conductivities to boundary integrals. Albuquerque et al. [18] extended the RIM to transform domain integrals into boundary integrals in a BEM formulation for anisotropic plate bending problems. Numerical results showed that the RIM, although more time-consuming, presents some advantages over the DRM in terms of accuracy and the absence of particular solutions in the formulation for static and dynamic problems. Gao et al. [19] also implemented the RIM to solve elastic problems with nonlinearly varying material parameters, such as for functionally graded materials and damage mechanics problems.

Another methodology for solving PDEs with variable coefficients is to use a parametrix (Levi function), which is usually available [20,21]. This allows a reduction of the mathematical problem to a boundary–domain integral or integro-differential equation (BDIE or BDIDE) [22–26]. AL-Jawary and Wrobel [22] have successfully implemented BDIE and BDIDE formulations for stationary heat transfer in isotropic materials with variable coefficients by using domain integrals. The numerical results show that high rates of convergence are obtained with mesh refinement. A pure BEM using the RIM has been derived and implemented in [23,24] to solve the two-dimensional Helmholtz equation and steady state heat conduction with variable coefficients, respectively.

A BDIE formulation and a BDIDE formulation for stationary heat transfer with variable coefficients are presented in [25] using specially constructed localized parametrices to reduce the BVP to a localized boundary–domain integral or integro-differential equation (LBDIE or LBDIDE). The use of specially constructed localized parametrices leads to sparsely populated systems of linear algebraic equations. An implementation of the LBDIE method for the numerical solution of a second-order linear elliptic PDE with variable coefficients is presented in [26], although the formulation is restricted to Neumann boundary-value problems.

Several numerical techniques have been proposed to generate boundary integral representations for the diffusion equation [27]. The DRM, initially applied to transient heat conduction problems by Wrobel et al. [28], interprets the time derivative in the diffusion equation as a body force and employs the fundamental solution to Laplace's equation to generate a BIE. Also, Wrobel and Brebbia [29] presented an extension of the DRM to deal with nonlinear diffusion problems in which the thermal conductivity, specific heat, and density coefficients are all functions of temperature.

Hematiyan and Karami [30] applied a meshless method as a boundary-only formulation for transient heat conduction with heat sources. The transformation of the domain integral into the corresponding boundary integral is carried out using Green's theorem.

Recent work by Yang and Gao [31] adopted the Green's function for the Laplace equation in deriving normalized BDIEs for time-dependent problems with varying heat conductivities. The authors argued that, unlike the standard BEM, considering the product of variable coefficients with the unknown functions as a new variable can provide accurate results. Then, the RIM is employed to convert the resulting domain integrals into equivalent boundary integrals. However, due to the way that they calculated the inner radial integral, the formulations still required calculating the integral inside the domain and this is restricted to star-shaped domains. Yang et al. [32] presented analytic integrations for the RIM for heat conduction problems with variable coefficients, which can reduce the time needed for computing the radial integrals.

Recently, a number of numerical techniques were developed aiming at decreasing the complexity of BEM algorithms from square to nearly linear. These are the fast multipole method [33], the wavelet transform [34], domain decomposition [35], adaptive cross-approximation [36] and hierarchical matrices [37], to name but a few. Application of these algorithms for compression and sparse storage of domain matrices was investigated for fluid flow problems by Ravnik et al. [34,38,39].

In this paper, a new type of boundary-only integral equation technique is developed for non-homogeneous transient heat conduction problems with variable coefficients based on the use of a parametrix. The RIM is used to convert the domain integrals appearing in both BDIE and BDIDE to equivalent boundary integrals. Rather than adopting the RIM available in the literature [31], in which the normalized temperature was used to formulate the integral equation, we adopt in our work the standard BDIE and new BDIDE methods to formulate the integral equation. Moreover, the radial integral is calculated only along the boundary. For domain integrals consisting of known functions the transformation is straightforward, while for domain integrals that include unknown variables the transformation is accomplished with the use of augmented RBFs, which is similar to the DRM approach. The most attractive feature of the method is that the transformations are very simple and have similar forms for two-dimensional and three-dimensional problems.

Furthermore, we propose a domain decomposition (subdomain) approach (SDBDIE), which results in a sparse system of equations, thus avoiding the need to calculate a large number of domain integrals. The discretization used in this paper leads to an overdetermined system of linear equations [40,41]. Some numerical examples are given to demonstrate the efficiency of the proposed methods.

2. Reduction of the diffusion equation to a BDIE/BDIDE

Let us consider the following diffusion equation in an isotropic non-homogeneous medium for a two-dimensional bounded body Ω, with prescribed temperature $\bar{u}(x)$ on the part $\partial_D\Omega$ of the boundary $\partial\Omega$ and prescribed heat flux $\bar{q}(x)$ on the remaining part $\partial_N\Omega$ of $\partial\Omega$, i.e. we consider the second-order linear parabolic PDE,

$$\sum_{i=1}^{2}\frac{\partial}{\partial x_i}\left[a(x)\frac{\partial u(x,t)}{\partial x_i}\right]=f(x,t)+D(x,t)\frac{\partial u(x,t)}{\partial t},\quad x\in\Omega \tag{1}$$

with the initial–boundary conditions

$$u(x_1,x_2,0)=u_0(x),\quad \text{for } (x_1,x_2)\in\Omega \tag{2}$$

$$u(x_1,x_2,t)=\bar{u}(x_1,x_2,t),\quad \text{for } (x_1,x_2)\in\partial_D\Omega,\ t>0 \tag{3}$$

$$Tu(x_1,x_2,t)=\bar{q}(x_1,x_2,t),\quad \text{for } (x_1,x_2)\in\partial_N\Omega,\ t>0 \tag{4}$$

where $u(x,t)$ is the temperature, $a(x)$ a known variable thermal conductivity coefficient, $f(x)$ a known heat source, T the surface flux operator, $x=(x_1,x_2)$,

$$[Tu](x,t):=a(x)\frac{\partial u(x,t)}{\partial x_i}n_i(x),\quad i=1,2,$$

$n_1(x)$ and $n_2(x)$ are the components of the external normal vector $n(x)$ to the boundary $\partial\Omega$, u_0, $\bar{u}$ and $\bar{q}$ are known functions, $D(x,t)=\rho c$, ρ is the mass density and c is the specific heat.

The Green formula for the differential operator L has the form

$$\int_\Omega[uL\varphi-\varphi Lu]d\Omega=\int_{\partial\Omega}[uT\varphi-\varphi Tu]d\Gamma \tag{5}$$

where u and φ are arbitrary functions.

Let L be a linear operator and $G(x,y)$ its fundamental solution, i.e.

$$L_xG(x,y)=\delta(x-y)$$

where $y=(y_1,y_2)$ is a source point, and δ is the Dirac delta function. Also, the fundamental solution used is the same as for Laplace's equation, given by

$$G(x,y)=\frac{1}{2\pi}\ln|x-y|, \tag{6}$$

where $|x-y|=\sqrt{(x_1-y_1)^2+(x_2-y_2)^2}$.

Then, one could take $\varphi(x)=G(x,y)$, identify $u(x)$ with a solution of Eq. (1), and thus arrive at the third Green identity

$$\begin{aligned}c(y)u(y,t)-\int_{\partial\Omega}[u(x,t)T_xG(x,y)-G(x,y)Tu(x,t)]d\Gamma(x)\\=\int_\Omega G(x,y)f(x,t)d\Omega(x)+\int_\Omega D(x,t)G(x,y)\frac{\partial u(x,t)}{\partial t}d\Omega(x)\end{aligned} \tag{7}$$

where

$$c(y)=\begin{cases}1 & \text{if } y\in\Omega\\ 0 & \text{if } y\notin\bar{\Omega}\\ \dfrac{\alpha(y)}{2\pi} & \text{if } y\in\partial\Omega \text{ and } \Omega\subset\mathbb{R}^2,\end{cases} \tag{8}$$

where $\alpha(y)$ is the interior angle at a point y of the boundary $\partial\Omega$. Substituting the boundary conditions in the Green identity equation (7) and applying it for $y \in \partial\Omega$, we arrive at a direct boundary integral equation [1,13].

For partial differential operators with variable coefficients, like L in Eq. (1), a fundamental solution is generally not available in explicit form. In order to get the third Green identity corresponding to the operator L with variable coefficients in Eq. (1), there are two approaches available in the literature.

The first approach is to use a parametrix, which is often available [20–26,42], and which is a function $P(x, y)$ satisfying the equation

$$L_x P(x, y) = \delta(x - y) + R(x, y), \tag{9}$$

where $R(x, y)$ is the remainder which has no more than a weak (integrable) singularity at $x = y$. The fundamental solution of the operator with "frozen coefficients" $a(x) = a(y)$ corresponding to the operator L defined in (1) can be used as a parametrix, in the two-dimensional case [22,25,26]:

$$P(x, y) = \frac{1}{2\pi a(y)} \ln|x - y|. \tag{10}$$

Substituting Eq. (10) in Eq. (9), the remainder $R(x, y)$ will then be [22,25,26]

$$R(x, y) = \sum_{i=1}^{2} \frac{x_i - y_i}{2\pi a(y)|x - y|^2} \frac{\partial a(x)}{\partial x_i}, \quad x, y \in \mathbb{R}^2. \tag{11}$$

Substituting $P(x, y)$ for $\varphi(x)$ in Eq. (5) and taking $u(x)$ as a solution to Eq. (1), we obtain the integral equality

$$\begin{aligned} &c(y)u(y, t) - \int_{\partial\Omega} [u(x, t)T_x P(x, y) - P(x, y)Tu(x, t)]d\Gamma(x) + \int_{\Omega} R(x, y)u(x, t)d\Omega(x) \\ &= \int_{\Omega} P(x, y)f(x, t)d\Omega(x) + \int_{\Omega} D(x, t)P(x, y)\frac{\partial u(x, t)}{\partial t}d\Omega(x). \end{aligned} \tag{12}$$

Now, we can multiply both sides of Eq. (12) by $a(y)$ to obtain

$$\begin{aligned} &a(y)c(y)u(y, t) - \int_{\partial\Omega} [u(x, t)T_x G(x, y) - G(x, y)Tu(x, t)]d\Gamma(x) + \int_{\Omega} \tilde{R}(x, y)u(x, t)d\Omega(x) \\ &= \int_{\Omega} G(x, y)f(x, t)d\Omega(x) + \int_{\Omega} D(x, t)G(x, y)\frac{\partial u(x, t)}{\partial t}d\Omega(x), \end{aligned} \tag{13}$$

where

$$G(x, y) = a(y)P(x, y) = \frac{1}{2\pi} \ln|x - y|, \qquad \tilde{R}(x, y) = a(y)R(x, y) = \sum_{i=1}^{2} \frac{x_i - y_i}{2\pi|x - y|^2} \frac{\partial a(x)}{\partial x_i}.$$

The second alternative approach also uses the fundamental solution G for the Laplace equation as a weighting function for Eq. (1), leading to [31]

$$\sum_{i=1}^{2} \int_{\Omega} \frac{\partial}{\partial x_i} \left[a(x) \frac{\partial u(x, t)}{\partial x_i} \right] G(x, y)d\Omega(x) = \int_{\Omega} f(x, t)G(x, y)d\Omega(x) + \int_{\Omega} D(x, t) \frac{\partial u(x, t)}{\partial t} G(x, y)d\Omega(x), \quad y \in \Omega. \tag{14}$$

Using integration by parts, the first domain integral in Eq. (14) can be written as

$$\begin{aligned} \sum_{i=1}^{2} \int_{\Omega} \frac{\partial}{\partial x_i} \left[a(x) \frac{\partial u(x, t)}{\partial x_i} \right] G(x, y)d\Omega(x) = \sum_{i=1}^{2} \Bigg[&\int_{\Omega} \frac{\partial}{\partial x_i} \left[G(x, y)a(x) \frac{\partial u(x, t)}{\partial x_i} \right] d\Omega(x) \\ &- \int_{\Omega} \frac{\partial G(x, y)}{\partial x_i} a(x) \frac{\partial u(x, t)}{\partial x_i} d\Omega(x) \Bigg]. \end{aligned} \tag{15}$$

The Gauss divergence theorem can be applied now to the first domain integral on the right-hand side, leading to

$$\int_{\Omega} \frac{\partial}{\partial x_i} \left[G(x, y)a(x) \frac{\partial u(x, t)}{\partial x_i} \right] d\Omega(x) = \int_{\partial\Omega} G(x, y)Tu(x, t)d\Gamma(x). \tag{16}$$

The second domain integral on the right-hand side of Eq. (15) can be manipulated as

$$\begin{aligned} -\sum_{i=1}^{2} \int_{\Omega} \frac{\partial G(x, y)}{\partial x_i} \left[a(x) \frac{\partial u(x, t)}{\partial x_i} \right] d\Omega(x) = &-\sum_{i=1}^{2} \int_{\Omega} \frac{\partial G(x, y)}{\partial x_i} \frac{\partial}{\partial x_i} [a(x)u(x, t)] d\Omega(x) \\ &+ \sum_{i=1}^{2} \int_{\Omega} \frac{\partial G(x, y)}{\partial x_i} \frac{\partial a(x)}{\partial x_i} u(x, t)d\Omega(x). \end{aligned} \tag{17}$$

The first domain integral on the right-hand side of Eq. (17) can be manipulated as before and Gauss's divergence theorem applied to yield

$$-\sum_{i=1}^{2}\int_{\Omega}\frac{\partial G(x,y)}{\partial x_i}\frac{\partial}{\partial x_i}\left[a(x)u(x,t)\right]d\Omega(x) = -\int_{\partial\Omega}u(x,t)T_xG(x,y)d\Gamma(x) + \sum_{i=1}^{2}\int_{\Omega}\frac{\partial}{\partial x_i}\left[\frac{\partial G(x,y)}{\partial x_i}\right]a(x)u(x,t)d\Omega(x). \tag{18}$$

As the fundamental solution is singular, the source point y is surrounded by a small circle of radius ϵ, and then the integrals are examined in the limit as $\epsilon \longrightarrow 0$, as discussed in detail in [2]. The second domain integral on the right-hand side of Eq. (18) vanishes, since the source point is excluded from the integration domain. During the limit procedure the first domain integral on the right-hand side of Eq. (18) produces an additional term $a(y)c(y)u(y)$. Substituting Eqs. (15)–(18) in Eq. (14), we get the same third Green identity as in Eq. (13).

The identity (13) can be used for formulating either a BDIE or a BDIDE, with respect to u and its derivatives (we still prefer to call the new formulations in the next sections BDIE and BDIDE for simplicity even if the identity (13) has a domain integral of the time derivative). Let us consider the two forms below.

2.1. The boundary–domain integral equation (BDIE)

Substituting the boundary conditions (3) and (4) into (13), introducing a new variable $q(x,t) = Tu(x,t)$ for the unknown flux on $\partial_D\Omega$ and using Eq. (13) at $y \in \Omega \cup \partial\Omega$ reduces Eq. (1) to the following BDIE for $u(x,t)$ at $x \in \Omega \cup \partial_N\Omega$ and $q(x,t)$ at $x \in \partial_D\Omega$:

$$c^0(y)u(y,t) - \int_{\partial_N\Omega}u(x,t)T_xG(x,y)d\Gamma(x) + \int_{\partial_D\Omega}G(x,y)q(x,t)d\Gamma(x) + \int_{\Omega}\tilde{R}(x,y)u(x,t)d\Omega(x) = \Psi^0(y,t), \quad y \in \Omega \cup \partial\Omega,\ t > 0 \tag{19}$$

where

$$\Psi^0(y,t) := [c^0(y) - a(y)c(y)]\bar{u}(y,t) + \Psi(y,t), \tag{20}$$

$$\Psi(y,t) := \int_{\partial_D\Omega}\bar{u}(x,t)T_xG(x,y)d\Gamma(x) - \int_{\partial_N\Omega}G(x,y)\bar{q}(x,t)d\Gamma(x) + \int_{\Omega}G(x,y)f(x,t)d\Omega(x) + \int_{\Omega}D(x,t)\frac{\partial u(x,t)}{\partial t}G(x,y)d\Omega(x), \tag{21}$$

and

$$c^0(y) = \begin{cases} 0 & \text{if } y \in \partial_D\Omega \\ a(y)c(y) & \text{if } y \in \Omega \cup \partial_N\Omega. \end{cases} \tag{22}$$

2.2. The boundary–domain integro-differential equation (BDIDE)

Using another approach, we can substitute the boundary conditions (3) and (4) into (13) but leave T as a differential flux operator acting on u on the Dirichlet boundary $\partial_D\Omega$ and use the following BDIDE:

$$a(y)c(y)u(y,t) - \int_{\partial_N\Omega}u(x,t)T_xG(x,y)d\Gamma(x) + \int_{\partial_D\Omega}G(x,y)Tu(x,t)d\Gamma(x) + \int_{\Omega}\tilde{R}(x,y)u(x,t)d\Omega(x) = \Psi(y,t), \quad y \in \Omega \cup \partial_N\Omega,\ t > 0. \tag{23}$$

3. Transformation of domain integrals to the boundary using RIM

In this section, the RIM [15–19,23,24,31,32] is used to transform the domain integrals appearing in Eqs. (19) and (23) into boundary integrals.

3.1. RIM formulation for domain integrals with known integrand

A domain integral with known integrand $f(x)$, $x = (x_1, x_2)$, can be transformed into an equivalent boundary integral by following the procedure given in detail in [15–19,23,24,31,32]:

$$\int_{\Omega} f(x)d\Omega = \int_{\partial\Omega} \frac{1}{r^{\alpha}} \frac{\partial r}{\partial n} F(x)d\Gamma(x), \tag{24}$$

where

$$F(x) = \int_0^{r(x)} f(x)r^{\alpha}dr. \tag{25}$$

In Eqs. (24) and (25), $\alpha = 1$ for the two-dimensional case and $\alpha = 2$ for the three-dimensional case.

The following remarks are important for the RIM:

- In order to evaluate the radial integral in Eq. (25), the coordinates x_1, x_2 in $f(x)$ need to be expressed in terms of the distance r using

$$x_i = y_i + r_{,i}r \quad i = 1, 2 \tag{26}$$

  where the quantities y_i and $r_{,i}$ are constant for the radial integral in Eq. (25), with $r_{,i} = \frac{x_i - y_i}{r}$.
- Following the idea presented in [43], we can introduce the change of variable

$$r = s|x - y|, \quad s \in [0, 1] \tag{27}$$

  and substitute the new transformation in the straight-line radial integral in Eq. (25), leading to

$$F(x) = \int_0^1 f(y_1 + r_{,1}rs, y_2 + r_{,2}rs)r^2 sds. \tag{28}$$

The representation (28) makes it unnecessary to define a variable transformation as in [17] to treat the radial integral in Eq. (25), adding an attractive feature to the RIM as Eq. (25) is now a pure boundary integral. Moreover, the star-shaped requirement for the integral in Eq. (25) can be relaxed as the straight path from the source point y to any field point x always exists [23,24,43].

3.1.1. Transformation of the heat source domain integral to the boundary

Both Eqs. (19) and (23) have domain integrals coming from the known heat source $f(x, t)$. The RIM can be directly used to convert these domain integrals to the boundary. This leads to

$$\int_{\Omega} G(x, y)f(x, t)d\Omega(x) = \int_{\partial\Omega} \frac{1}{r} \frac{\partial r}{\partial n} F(x, t)d\Gamma(x) \tag{29}$$

where

$$F(x, t) = \int_0^1 G(x, y)f(y_1 + r_{,1}rs, y_2 + r_{,2}rs, t)r^2 sds. \tag{30}$$

The integral in Eq. (30) can be calculated analytically for many different functions [23,24], and numerically without the need to define a transformation as in [14,15]. Also, due to the radial integral in Eq. (30), the weak singularity coming from the fundamental solution is removed.

3.2. RIM formulation for domain integrals with unknown integrand

3.2.1. RIM formulation for left-hand side domain integrals with unknown integrand

As the last domain integrals on the left-hand side of Eqs. (19) and (23) have the unknown temperature $u(x, t)$, the RIM in Eqs. (29) and (30) cannot be directly used. However, $u(x, t)$ can be approximated by radial basis functions (RBFs) [13,17,24,44]. We adopt an augmented RBF, as discussed in [17,24,44].

Let us approximate the temperature $u(x, t)$ in the following way:

$$u(x, t) = \sum_{k=1}^{M} \alpha_k \phi_k(R) + c_1x_1 + c_2x_2 + c_3 \tag{31}$$

where $M = N_b + N_I$ and N_b, N_I are the number of boundary and interior nodes, respectively. It is known that the RBFs augmented by a linear polynomial with interior nodes produce better results in comparison to the case without the interior nodes; therefore interior nodes will be used in the current work. The coefficients α_k for $k = 1, \ldots, M$, c_1, c_2 and c_3 depend

on time t. Also, $R = \|x - a\|$ is the distance from the application point a to the field point x. Normally, the application points a consist of all boundary nodes and some selected interior nodes.

The following equilibrium conditions have to be satisfied [45]:

$$\sum_{k=1}^{M} \alpha_k = \sum_{k=1}^{M} \alpha_k x_{1k} = \sum_{k=1}^{M} \alpha_k x_{2k} = 0 \tag{32}$$

where x_{1k}, x_{2k} are the coordinates of each of the M field points. The unknown coefficients α_k, c_1, c_2 and c_3 can be calculated by applying Eqs. (31) and (32) at the application points a, as discussed in detail in [23,24].

Substituting Eq. (31) into the last domain integral on the left-hand side of both Eqs. (19) and (23), we obtain

$$\int_{\Omega} \tilde{R}(x, y)u(x, t)d\Omega(x) = \int_{\partial\Omega} Q(x, t)d\Gamma(x), \tag{33}$$

where the calculation of the boundary integral $\int_{\partial\Omega} Q(x, t)d\Gamma(x)$ is discussed in detail in [24].

In this paper, $\phi(R) = R^3$ is adopted and expressed in terms of the distance r as discussed in [24]. After numerical integration, the unknown coefficients α_k, $k = 1, \ldots, M$, c_1, c_2 and c_3 can be calculated following the procedures discussed in [23,24].

3.2.2. RIM formulation for right-hand side domain integrals with unknown integrand

Eqs. (19) and (23) have the unknown temperature–time derivative $\frac{\partial u(x,t)}{\partial t}$ in the last domain integral of Eq. (21), and the RIM in Eqs. (29) and (30) cannot be directly used. We adopt a procedure similar to that used previously, as follows:

Let us approximate the variation of $\frac{\partial u(x,t)}{\partial t}$ in the following way:

$$\frac{\partial u(x, t)}{\partial t} = \sum_{k=1}^{M} \beta_k \phi_k(R) + d_1 x_1 + d_2 x_2 + d_3 \tag{34}$$

where the coefficients β_k for $k = 1 \ldots M$, d_1, d_2 and d_3 depend on time t.

The following equilibrium conditions have to be satisfied, as before:

$$\sum_{k=1}^{M} \beta_k = \sum_{k=1}^{M} \beta_k x_{1k} = \sum_{k=1}^{M} \beta_k x_{2k} = 0. \tag{35}$$

Substituting Eq. (34) into the last domain integrals of Eq. (21), we obtain

$$\begin{aligned}\int_{\Omega} D(x, t)\frac{\partial u(x, t)}{\partial t}G(x, y)d\Omega(x) &= \sum_{k=1}^{M} \beta_k \int_{\Omega} D(x, t)G(x, y)\phi_k(R)d\Omega(x) \\ &+ d_1 \int_{\Omega} D(x, t)G(x, y)x_1 d\Omega(x) + d_2 \int_{\Omega} D(x, t)G(x, y)x_2 d\Omega(x) + d_3 \int_{\Omega} D(x, t)G(x, y)d\Omega(x).\end{aligned} \tag{36}$$

It is very important that, before applying the RIM, the coordinates x_1 and x_2 appearing in Eq. (36) are expressed in terms of the distance r using Eq. (26). Now, applying the RIM to each domain integral in Eq. (36) leads to

$$\int_{\Omega} D(x, t)\frac{\partial u(x, t)}{\partial t}G(x, y)d\Omega(x) = \int_{\partial\Omega} b(x, t)d\Gamma(x),$$

where

$$\begin{aligned}\int_{\partial\Omega} b(x, t)d\Gamma(x) &= \sum_{k=1}^{M} \beta_k \int_{\partial\Omega} \frac{1}{r}\frac{\partial r}{\partial n}\acute{F}1(x, t)d\Gamma(x) + d_1 \int_{\partial\Omega} \frac{1}{r}\frac{\partial r}{\partial n}\acute{F}2(x, t)d\Gamma(x) \\ &+ d_2 \int_{\partial\Omega} \frac{1}{r}\frac{\partial r}{\partial n}\acute{F}3(x, t)d\Gamma(x) + d_3 \int_{\partial\Omega} \frac{1}{r}\frac{\partial r}{\partial n}\acute{F}4(x, t)d\Gamma(x)\end{aligned} \tag{37}$$

where

$$\acute{F}1(x, t) = \int_0^1 D(x, t)G(x, y)\phi(R)r^2 sds, F2(x, t) = \int_0^1 D(x, t)G(x, y)(y_1 + r_{,1}rs)r^2 sds, \tag{38a}$$

$$\acute{F}3(x, t) = \int_0^1 D(x, t)G(x, y)(y_2 + r_{,2}rs)r^2 sds, F4(x, t) = \int_0^1 D(x, t)G(x, y)r^2 sds. \tag{38b}$$

After numerical integration, the unknown coefficients β_k, $k = 1, \ldots, M$, d_1, d_2 and d_3 can be calculated following the procedures discussed in [23,24].

4. The radial integration boundary integral and integro-differential equation (RIBIE/RIBIDE)

Eqs. (29)–(30), (33) and (37)–(40) can now be substituted in both the BDIE in Eq. (19) and the BDIDE in Eq. (23), leading to the following expressions.

4.1. The radial integration boundary integral equation (RIBIE)

$$c^0(y)u(y,t) - \int_{\partial_N\Omega} u(x,t)T_xG(x,y)d\Gamma(x) + \int_{\partial_D\Omega} G(x,y)q(x,t)d\Gamma(x) + \int_{\partial\Omega} Q(x,t)d\Gamma(x) = \Psi^0(y,t), \quad y \in \Omega \cup \partial\Omega, t > 0 \tag{39}$$

where Ψ^0 is given by Eq. (20) and

$$\Psi(y,t) := \int_{\partial_D\Omega} \bar{u}(x,t)T_xG(x,y)d\Gamma(x) - \int_{\partial_N\Omega} G(x,y)\bar{q}(x,t)d\Gamma(x) + \int_{\partial\Omega} b(x,t)d\Gamma(x) + \int_{\partial\Omega} \frac{1}{r}\frac{\partial r}{\partial n}F(x,t)d\Gamma(x). \tag{40}$$

4.2. The radial integration boundary integro-differential equation (RIBIDE)

$$a(y)c(y)u(y,t) - \int_{\partial_N\Omega} u(x,t)T_xG(x,y)d\Gamma(x) + \int_{\partial_D\Omega} G(x,y)Tu(x,t)d\Gamma(x) + \int_{\partial\Omega} Q(x,t)d\Gamma(x) = \Psi(y,t), \quad y \in \Omega \cup \partial_N\Omega, t > 0. \tag{41}$$

It can be seen clearly from both the RIBIE in Eq. (39) and the RIBIDE in Eq. (41) that all integrations are now carried out only on the boundary, with no domain integrals.

4.3. Discretization of the RIBIE

The RIBIE formulation employs mixed boundary elements with linear interpolation for u and constant interpolation for q to avoid the discontinuities of q at corner points. In this case, collocation was taken at the end points of each boundary element, since our previous researches have shown that end-node collocation generally provides higher accuracy than mid-node collocation [22–24]. It is important to point out that using end-node collocation will provide more equations than unknowns as discussed in Section 5.

To obtain a system of linear algebraic equations from the RIBIE (39), we collocate at the nodes $x^i, i = 1, \ldots, J$. We arrive at the following system of J linear algebraic equations for J unknowns $u(x^j,t)$, $x^j \in \Omega \cup \partial_N\Omega$ and $q(x^j,t) = (Tu)(x^j,t)$, $x^j \in \partial_D\Omega$:

$$c^0(x^i)u(x^i,t) + \sum_{x^j\in\Omega\cup\partial_N\Omega} K_{ij}u(x^j,t) + \sum_{x^j\in\partial_D\Omega} Q'_{ij}q(x^j,t) = \Psi^0(x^i,t) - \sum_{x^j\in\partial_D\Omega} K_{ij}\bar{u}(x^j,t), x^i \in \Omega \cup \partial\Omega, \quad i = 1,\ldots,J, \text{ no sum in } i, \tag{42}$$

where $\Psi^0(x^i,t)$ is calculated from Eq. (20), and

$$\Psi(x^i,t) = \int_{\partial_D\Omega} \bar{u}(x,t)T_xG(x,x^i)d\Gamma(x) - \int_{\partial_N\Omega} G(x,x^i)\bar{q}(x,t)d\Gamma(x) + \int_{\partial\Omega} b(x,t)d\Gamma(x) + \int_{\partial\Omega} \frac{1}{r}\frac{\partial r}{\partial n}F(x,t)d\Gamma(x), \tag{43}$$

$$K_{ij} = \int_{\partial\Omega} Q(x,t)d\Gamma(x) - \int_{\partial_N\Omega} \phi_j(x,t)T_xG(x,x^i)d\Gamma(x), \tag{44}$$

$$Q'_{ij} = \int_{\partial_D\Omega} G(x,x^i)v_j(x,t)d\Gamma(x) \tag{45}$$

where ϕ_j and v_j are linear and constant boundary interpolation functions, respectively.

4.4. Discretization of the RIBIDE

To obtain a system of linear algebraic equations from the RIBIDE (41), we collocate at the nodes x^i, $i = 1, \ldots, J$, and substitute a linear interpolation of $u(x, t)$ of the form

$$u(x,t) \approx \sum_{S_j \ni x} u(x^j, t)\Phi_j(x), \qquad \Phi_j(x) = \begin{cases} \phi_{kj}(x) & \text{if } x, x^j \in \bar{T}_k \\ 0 & \text{otherwise,} \end{cases} \tag{46}$$

where S_j in this case is the set of collocation points in $\partial_D\Omega$ and some selected interior nodes near the boundary segments; $\phi_{kj}(x, t)$ are the shape functions which can be constructed from the distance between the two end nodes of each segments and the selected interior nodes, and associated with the node x^j. In this work, the $\phi_{kj}(x)$ are chosen as piecewise linear functions.

We then arrive at a system of $J - J_D$ algebraic equations for $J - J_D$ unknowns $u(x^j, t)$, $x^j \in \Omega \cup \partial_N\Omega$. Substituting interpolation formulae (46) into the RIBIDE (41) leads to the following system of equations:

$$a(x^i)c(x^i)u(x^i,t) + \sum_{x^j \in \Omega \cup \partial_N\Omega} K'_{ij}u(x^j) = \Psi(x^i,t) - \sum_{x^j \in \partial_D\Omega} K'_{ij}\bar{u}(x^j,t), \quad x^i \in \Omega \cup \partial_N\Omega, \text{ no sum in } i, \tag{47}$$

where

$$K'_{ij} = K_{ij} + \int_{\partial_D\Omega} G(x, x^i)T\Phi_j(x)d\Gamma(x). \tag{48}$$

The calculation of the integral in Eq. (48) is presented in detail in [24]. The advantages of the RIBIDE technique are that the only boundary variables are those of u along Neumann boundaries, as there is no need for collocation along Dirichlet boundaries. Thus, the problem caused by the discontinuity of the normal derivative at corner points is avoided. Second, the system of linear equations is smaller than the one for RIBIE. This feature will save memory and computational time when we apply the RIBIDE for practical problems. Finally, the assembly of the system of equations is much easier than in the RIBIE, as discussed in [22–24].

5. Implementation and a time marching solution scheme

5.1. Assembling the system for RIBIE for diffusion with variable coefficients

Let us consider the RIBIE in Section 4.1 before applying the boundary conditions:

$$\begin{aligned} &a(y)c(y)u(y,t) - \int_{\partial\Omega} u(x,t)T_xG(x,y)d\Gamma(x) + \int_{\partial\Omega} G(x,y)q(x,t)d\Gamma(x) + \int_{\partial\Omega} Q(x,t)d\Gamma(x) \\ &\quad = \int_{\partial\Omega} \frac{1}{r}\frac{\partial r}{\partial n}F(x,t)d\Gamma(x) + \int_{\partial\Omega} b(x,t)d\Gamma(x), \quad y \in \Omega \cup \partial\Omega, t > 0. \end{aligned} \tag{49}$$

Let us start with a mesh of eight boundary elements and nine nodes, as shown in Fig. 1. For the RIBIE method, the system of algebraic equations resulting from Eq. (49) has two unknown variables q and u, i.e. q on Dirichlet boundaries and u on Neumann boundaries, in addition to u at interior nodes. After carrying out the numerical integrations for all boundary integrals in Eq. (49), we obtain the following system for the simple mesh in Fig. 1:

$$(\text{Hmatrix} + \text{Rmatrix})_{9\times 9} * u_{9\times 1} + (\text{Gmatrix})_{9\times 8} * q_{8\times 1} = \text{fvector}_{9\times 1} + (\text{Ematrix})_{9\times 9} * \dot{u}_{9\times 1} \tag{50}$$

where $\text{Hmatrix} = a(y)c(y)u(y,t) - \int_{\partial\Omega} u(x,t)\frac{\partial G(x,y)}{\partial n(x)}d\Gamma(x)$, Rmatrix is the last boundary integral on the left-hand side of Eq. (49), Gmatrix is the second boundary integral in Eq. (49) and fvector is the right-hand heat source vector. The Ematrix results from the boundary integral $\int_{\partial\Omega} Q(x,t)d\Gamma(x)$ given in Eq. (32).

Assume, in Fig. 1, that the top and bottom of the plate have Dirichlet boundary conditions, left and right have Neumann boundary conditions. Referring to Fig. 1, we have six known values of u, namely $u1, u4, u7, u3, u6, u9$ and four known values of q, namely $q1, q5, q4, q8$; also, we have three unknown values of u, namely $u2, u5, u8$ and four unknown values of q, namely $q2, q3, q6, q7$.

To solve Eq. (50), we adopt a time marching scheme [13,27,46]. A finite difference approximation for the time derivative term is given by

$$\dot{u} = \frac{u^{k+1} - u^k}{\Delta t}, \tag{51}$$

$$u = (1 - \theta_u)u^k + \theta_u u^{k+1}, \tag{52}$$

$$q = (1 - \theta_q)q^k + \theta_q q^{k+1}, \tag{53}$$

$$b = (1 - \theta_b)b^k + \theta_b b^{k+1}, \tag{54}$$

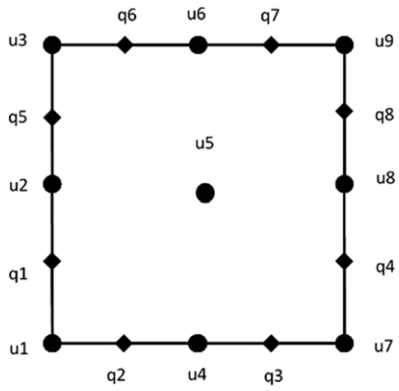

Fig. 1. Simple mesh with ∘ for u and ⋄ for flux q.

where Δt is the time step, u^k and q^k are the temperature and flux at the kth time step, and θ is a real parameter that determines whether the method is explicit ($\theta_u, \theta_q, \theta_b = 0$) or implicit ($\theta_u, \theta_q, \theta_b = 1$). The special choice of ($\theta_u, \theta_q, \theta_b = \frac{1}{2}$) is known as the Crank–Nicolson scheme. Several tests were done here to choose the best values for θ and we selected $\theta_u = \frac{1}{2}$, $\theta_q = 1$ and $\theta_b = 1$.

By applying the values of $\theta_u, \theta_q, \theta_b$ and Eqs. (51)–(53) in Eq. (50), we get

$$\left[\frac{1}{2}(\text{Hmatrix} + \text{Rmatrix})_{9\times 9} - \frac{1}{\Delta t}(\text{Ematrix})_{9\times 9}\right] * u^{k+1}_{9\times 1} + (\text{Gmatrix})_{9\times 8} * q^{k+1}_{8\times 1}$$
$$= \text{fvector}_{9\times 1} + \left[-\frac{1}{2}(\text{Hmatrix} + \text{Rmatrix})_{9\times 9} - \frac{1}{\Delta t}(\text{Ematrix})_{9\times 9}\right] * u^{k}_{9\times 1}. \tag{55}$$

Now we can define the boundary conditions and by moving the columns corresponding to the known u and q values to the right-hand side and rearranging the system, we get

$$A_{9\times 7} * x^{k+1}_{7\times 1} = \text{fvector}^{k+1}_{9\times 1} + \left[-\frac{1}{2}(\text{Hmatrix} + \text{Rmatrix})_{9\times 9} - \frac{1}{\Delta t}(\text{Ematrix})_{9\times 9}\right] * u^{k}_{9\times 1} =: B^{k+1}_{9\times 1}. \tag{56}$$

In [22–24,42], the least squares technique has been applied in the following way, the final system being $Cx = d$:

$$[C]_{7\times 7} = [A^{tr}]_{7\times 9}[A]_{9\times 7}, \quad \text{and} \quad [d]_{7\times 1} = [A^{tr}]_{7\times 9}[B]_{9\times 1}.$$

The disadvantages of setting up the normal equations ($A^{tr}A$) are discussed in [47–49]:

(1) Normal equations square the condition number of the original system of equations.
(2) Setting up the normal equations can lead to loss of accuracy.
(3) Setting up the normal equations is costly in terms of cpu time and memory storage.
(4) The possible sparsity of the original set of equations is lost with the normal equations (in our work, the matrix A is already dense for both the RIBIE and the RIBIDE).

In order to avoid all these difficulties, MATLAB avoids calculating the normal equations. There are several ways to compute the unknown quantities x:

(1) The backslash operator not only solves square, nonsingular systems by Gaussian elimination, but it also computes the least squares solution to rectangular, overdetermined systems:

$$x = A \setminus B.$$

The computation is done by QR factorization.
(2) Statistics Toolbox functions like regress and regstats call the MATLAB backslash operator to perform linear regression. The QR decomposition is also used for an efficient computation (see [50,51]):

$$x = \text{regress}(B, A).$$

In the time marching computation, the unknown quantities x are updated at each time step by the new values obtained after solving Eq. (56). At the first time, the temperature and heat flux at all boundary and internal points are specified with initial values. The computation ends when all time steps are fulfilled [31] or a steady state is reached.

5.2. Assembling the system for RIBIDE for diffusion with variable coefficients

Let us recall the RIBIDE in Section 4.2, given by Eq. (41). By following exactly the same procedure as for steady-state heat conduction and the Helmholtz equation with variable coefficients in [22–24,42] for the integro-differential equation method, the unknown is only u in Neumann boundaries, in addition to interior nodes, namely $u2$, $u5$, $u8$. Therefore, the implementation here is much simpler than the RIBIE. Several tests were done again to choose the best values for θ and we concluded the values to be the same as for RIBIE, i.e. $\theta_u = \frac{1}{2}$ and $\theta_b = 1$. We then get

$$\left[\frac{1}{2}(\text{Hmatrix} + \text{Rmatrix} + \text{Gmatrix})_{3\times3} - \frac{1}{\Delta t}(\text{Ematrix})_{3\times3}\right] * u^{k+1}_{3\times1} = b^{k+1}_{3\times1} + \left[-\frac{1}{2}(\text{Hmatrix} + \text{Rmatrix} + \text{Gmatrix})_{3\times3} - \frac{1}{\Delta t}(\text{Ematrix})_{3\times3}\right] * u^{k}_{3\times1}. \tag{57}$$

The unknown quantities u can be obtained from

$$u^{k+1}_{3\times1} = M \setminus S,$$

where $M = \left[\frac{1}{2}(\text{Hmatrix} + \text{Rmatrix} + \text{Gmatrix})_{3\times3} - \frac{1}{\Delta t}(\text{Ematrix})_{3\times3}\right]$ and $S = b^{k+1}_{3\times1} + \left[-\frac{1}{2}(\text{Hmatrix} + \text{Rmatrix} + \text{Gmatrix})_{3\times3} - \frac{1}{\Delta t}(\text{Ematrix})_{3\times3}\right] * u^{k}_{3\times1}$.

In the time marching computation, the unknown quantities u are updated at each time step by using the new values obtained after solving Eq. (57) (using the same solver as in previous subsection, since the system is square the backslash operator uses the Gauss elimination method to solve for the unknown u). At the first time step, the temperatures at all Neumann boundary and internal points are specified with initial values.

6. The subdomain approach — SDBDIE

A subdomain (or macro-element) approach to the BDIE method has been used to simulate fluid flow phenomena. Ramšak and Škerget [40] used it with the stream function–vorticity formulation of the Navier–Stokes equations, and Ravnik et al. [38,41] used it with the velocity–vorticity formulation. The discretization used in these works led to an overdetermined system of linear equations, which was solved in a least squares manner. In the present work, we extend the approach proposed by Ravnik et al. [41] for problems with variable coefficients.

In the subdomain approach the whole domain Ω is divided into subdomains Ω_i, where $\sum \Omega_i = \Omega$. The subdomains used are rectangular cells. The boundary of each subdomain is denoted by $\partial\Omega_i$. The governing integral equation (13) can be written for each subdomain as

$$a(y)c(y)u(y,t) - \int_{\partial\Omega_i}[u(x,t)T_xG(x,y) - G(x,y)q(x,t)]d\Gamma(x) + \int_{\Omega_i}\tilde{R}(x,y)u(x,t)d\Omega(x) = \int_{\Omega_i}G(x,y)f(x,t)d\Omega(x) + \int_{\Omega_i}D(x,t)\frac{\partial u(x,t)}{\partial t}G(x,y)d\Omega(x). \tag{58}$$

The partial derivative over time is approximated by a second-order finite difference scheme, given as

$$\dot{u} \approx \frac{3u^{k+1} - 4u^k + u^{k-1}}{2\Delta t}, \tag{59}$$

where the discrete version of the partial time derivative depends on the time step Δt, the function in the next time step u^{k+1}, the function in the current time step u^k and the function in the previous time step u^{k-1}. The implicit method is used with $u = u^{k+1}$. With this approximation, Eq. (58) may be rewritten as

$$a(y)c(y)u(y,t) - \int_{\partial\Omega_i}[u(x,t)T_xG(x,y) - G(x,y)q(x,t)]d\Gamma(x) + \int_{\Omega_i}\left(\tilde{R}(x,y) - \frac{3}{2\Delta t}D(x,t)G(x,y)\right)u(x,t)d\Omega(x) = \int_{\Omega_i}G(x,y)\left(f(x,t) + \frac{-4u^k(x) + u^{k-1}(x)}{2\Delta t}D(x,t)\right)d\Omega(x). \tag{60}$$

In each subdomain, nodes are located at the corners and on the centres of sides, plus an additional node in the centre of the subdomain. This enables quadratic interpolation of the unknown function. In order to avoid the singularity of the normal derivative at corners, the flux points are set into the subdomain side. Linear interpolation of fluxes is used. The source point y is collocated at all function and flux nodes.

Setting up the linear system of equations requires the following boundary integrals to be calculated:

$$H^i_j(y) = \int_{\partial\Omega_i}\varphi_j(x)T_xG(x,y)d\Gamma(x), \qquad G^i_j(y) = \int_{\partial\Omega_i}\phi_j(x)G(x,y)d\Gamma(x), \tag{61}$$

where φ_j and ϕ_j are quadratic and linear boundary interpolation functions, respectively. In addition, the following domain integrals are required:

$$B_j^i(y) = \int_{\Omega_i} \Phi_j(x) G(x, y) d\Omega(x), \qquad V_j^i(y) = \int_{\Omega_i} \Phi_j(x) \tilde{R}(x, y) d\Omega(x), \tag{62}$$

where the Φ_j are quadratic domain interpolation functions. Integration is performed using the Gaussian quadrature rule with 48 points. A polar coordinate system transformation is used to handle weakly singular integrals. Calculation of the free coefficient $c(y)$ is performed indirectly. An analytical solution of the rigid body movement problem is used to find the diagonal terms of the system matrix, using the values of other integrals.

Since subdomains are used, the total number of integrals that need to be calculated scales as $\mathcal{O}(nN)$, where n is the number of nodes per subdomain and N is the number of subdomains. Since n is a small number, depending on the interpolation scheme that we chose for the function and its flux, we can state that the memory cost scales linearly with the number of nodes in the domain. This is a major improvement over the classical approach, where the memory cost scales quadratically with the number of nodes.

The discrete system of linear equation for one subdomain is

$$[c]\{u\} - [H]\{u\} + [G]\{q\} + \left([V] - \frac{3}{2\Delta t}\{D\}[B]\right)\{u\} = [B]\left(\{f\} + \{D\}\frac{-4\{u^k\} + \{u^{k-1}\}}{2\Delta t}\right), \tag{63}$$

where square brackets represent matrices and curly bracket vectors represent nodal values.

Between neighbouring subdomains, which share some of the nodes, compatibility conditions are prescribed, i.e. the function value at the node which is shared by subdomains is equal for all subdomains. For two subdomains which share a face, the flux through this face has the same value but opposite sign. Compatibility conditions lead to an overdetermined system of equations, since the number of unknowns is smaller than the number of equations. The overdetermined system is solved in a least squares manner [41].

7. Numerical results

In this section, we shall examine some test examples in order to assess the performance of the proposed formulations. We apply the RIBIDE/RIBIE and SDBDIE for homogeneous, non-homogeneous and variable coefficient diffusion equations on a square domain, for which an exact analytical solution, u_{exact}, is available. The RBF $\phi(R) = R^3$ is adopted for the RIBIDE/RIBIE in all test examples. Also, the top and bottom sides of the plates for all test examples have prescribed temperature u (Dirichlet boundary conditions), while the left and right are imposed with heat flux q (Neumann boundary conditions). The root mean square (RMS) error is calculated to check the convergence of the proposed methods:

$$RMS(J) = \left(\frac{\sum_{j=1}^{J} (u_{approx,j} - u_{exact,j})^2}{\sum_{j=1}^{J} u_{exact,j}^2} \right)^{1/2}, \tag{64}$$

where u_{approx} is the numerical solution and J is the number of nodes in the computational mesh. The error has been calculated for $J = 9, 25, 81, 289$ and 1089 and the time interval $0 < t < 1$ has been adopted in all test examples.

7.1. Numerical results for the homogeneous diffusion equation with constant $a(x)$

7.1.1. Test 1

Consider a square domain, $\Omega = [0, 1]^2$. The value of $D(x, t)$ is set as constant, $D(x, t) = 1$, and $f(x, t) = 0$. Initially, at $t = 0$, the scalar field function $u(x_1, x_2, t)$ has the form

$$u(x_1, x_2, 0) = 1 + \cos\left(\frac{\pi}{4}x_1\right)\sin\left(\frac{\pi}{4}x_2\right).$$

The following time-dependent mixed boundary conditions are applied on the square domain:

$$u(x_1, 0, t) = 1, \qquad u(x_1, 1, t) = 1 + e^{-\frac{\pi^2}{8}t}\cos\left(\frac{\pi}{4}x_1\right)\sin\left(\frac{\pi}{4}\right),$$
$$\frac{\partial u(0, x_2, t)}{\partial n} = 0, \qquad \frac{\partial u(1, x_2, t)}{\partial n} = -\frac{\pi}{4}e^{-\frac{\pi^2}{8}t}\sin\left(\frac{\pi}{4}\right)\sin\left(\frac{\pi}{4}x_2\right).$$

The exact solution of this problem is $u(x_1, x_2, t) = 1 + e^{-\frac{\pi^2}{8}t}\cos\left(\frac{\pi}{4}x_1\right)\sin\left(\frac{\pi}{4}x_2\right)$.

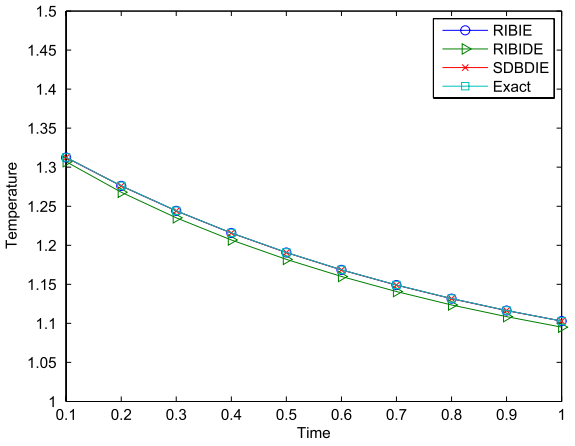

Fig. 2. Temperature distribution $u(0.5, 0.5, t)$.

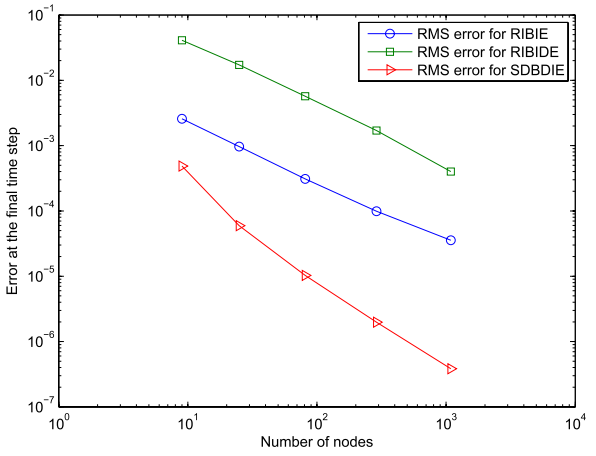

Fig. 3. RMS error for RIBIE, RIBIDE and SDBDIE methods for test 1 with $\Delta t = 0.01$.

Fig. 2 shows the variation of $u(0.5, 0.5, t)$ as a function of time t obtained using RIBIE, RIBIDE and SDBDIE with $\Delta t = 0.01$. The total number of nodes is fixed to 81 (32 on the boundary plus 49 in the interior). It can be seen that all the methods are able to generate accurate solutions in good agreement with the exact solution.

Moreover, Fig. 3 plots the RMS error for RIBIE, RIBIDE and SDBDIE versus the number of nodes. The SDBDIE yields lowest errors in comparison to the RIBIE and RIBIDE due to the use of a quadratic \ linear interpolation scheme, compared to a linear \ constant interpolation for the RIBIE and the RIBIDE. The SDBDIE also employs a time marching scheme of higher order.

7.2. Numerical results for the non-homogeneous diffusion equation with constant $a(x)$

7.2.1. Test 2

Consider a square domain, $\Omega = [1, 2]^2$. The value of $D(x, t)$ is set as constant, $D(x, t) = \frac{1}{6}$, and $f(x, t) = 6(x_1 + x_2) - 2t$. Initially, at $t = 0$, the scalar field function $u(x_1, x_2, t)$ is given by

$$u(x_1, x_2, 0) = x_1^3 + x_2^3.$$

The following time-dependent mixed boundary conditions are applied on the square domain:

$$u(x_1, 1, t) = x_1^3 + 1 + 6t^2, \qquad u(x_1, 2, t) = x_1^3 + 8 + 6t^2,$$
$$\frac{\partial u(1, x_2, t)}{\partial n} = -3, \qquad \frac{\partial u(2, x_2, t)}{\partial n} = 12.$$

The exact solution of this problem is $u(x_1, x_2, t) = x_1^3 + x_2^3 + 6t^2$. Fig. 4 plots the RMS error for the final time step for RIBIE, RIBIDE and SDBDIE. In both cases we observe good convergence properties for all methods. Again, we observe that SDBDIE provides the best results. It can be clearly seen that the RIBIE gives better results than the RIBIDE due to the term $T\Phi_j(x)$ in the RIBIDE being constant within each element, as discussed in detail in [22–24].

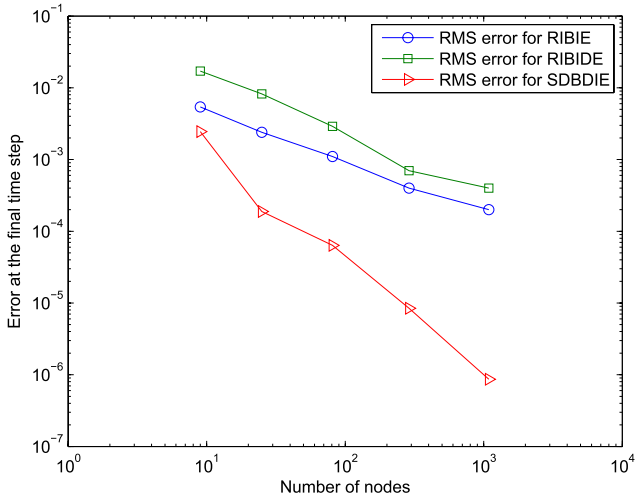

Fig. 4. RMS error for RIBIE, RIBIDE and SDBDIE methods for test 2 with $\Delta t = 0.1$.

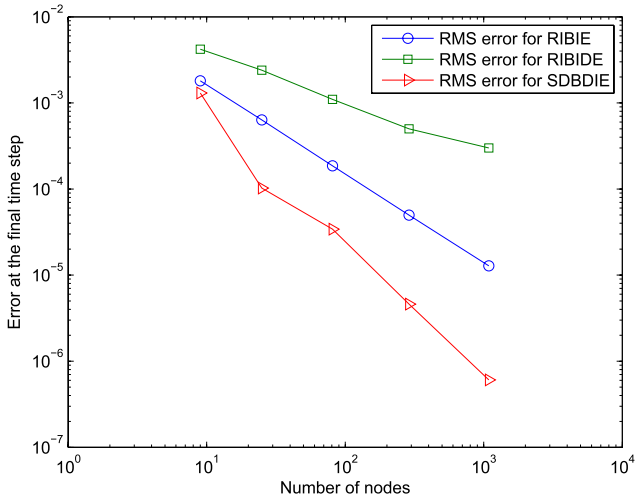

Fig. 5. RMS error for RIBIE, RIBIDE and SDBDIE methods for test 3 with $\Delta t = 0.1$.

7.3. Numerical results for the non-homogeneous diffusion equation with variable $a(x)$

7.3.1. Test 3

Consider a square domain, $\Omega = [1, 2]^2$. The value of $D(x, t)$ is set as constant, $D(x, t) = 1, f(x, t) = 6(x_1 + x_2) - 4$ and $a(x) = x_1 + x_2$. Initially, at $t = 0$, the scalar field function $u(x_1, x_2, t)$ has the form

$$u(x_1, x_2, 0) = x_1^2 + x_2^2.$$

The following time-dependent mixed boundary conditions are applied on the square domain:

$$u(x_1, 1, t) = x_1^2 + 1 + 4t, \qquad u(x_1, 2, t) = x_1^2 + 4 + 4t,$$
$$\frac{\partial u(1, x_2, t)}{\partial n} = -2(1 + x_2), \qquad \frac{\partial u(2, x_2, t)}{\partial n} = 4(2 + x_2).$$

The exact solution of this problem is $u(x_1, x_2, t) = x_1^2 + x_2^2 + 4t$. Fig. 5 plots the RMS error for the final time step for RIBIE, RIBIDE and SDBDIE. It can be clearly seen that on increasing the number of nodes the accuracy increases and the RMS error is reduced for all methods.

7.3.2. Test 4

Consider a square domain, $\Omega = [1, 2]^2$. The value of $D(x, t)$ is set as variable, $D(x, t) = x_1 + x_2, f(x, t) = 5(x_1 + x_2)$ and $a(x) = x_1 + x_2$. Initially, at $t = 0$, the scalar field function $u(x_1, x_2, t)$ is given by

$$u(x_1, x_2, 0) = x_1^2 + x_2^2.$$

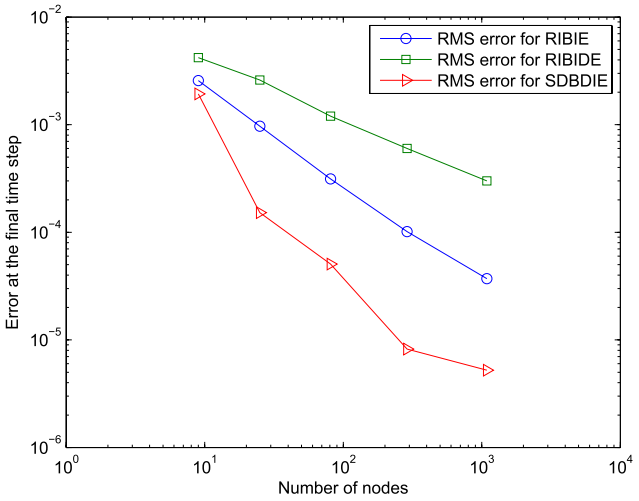

Fig. 6. RMS error for RIBIE, RIBIDE and SDBDIE methods for test 4 with $\Delta t = 0.1$.

The following time-dependent mixed boundary conditions are applied on the square domain:

$$u(x_1, 1, t) = x_1^2 + 1 + t, \qquad u(x_1, 2, t) = x_1^2 + 4 + t,$$
$$\frac{\partial u(1, x_2, t)}{\partial n} = -2(1 + x_2), \qquad \frac{\partial u(2, x_2, t)}{\partial n} = 4(2 + x_2).$$

The exact solution of this problem is $u(x_1, x_2, t) = x_1^2 + x_2^2 + t$. Test 4 presents a problem with material parameters $a(x)$ and $D(x, t)$ variable. Fig. 6 shows that, by fixing the time step to $\Delta t = 0.1$ and increasing the number of nodes, we achieved satisfactory results and convergence for all methods.

7.3.3. Test 5

Consider a square domain, $\Omega = [1, 2]^2$. The value of $D(x, t)$ is set as variable, $D(x, t) = 1 + t, f(x, t) = 9(x_1^2 + x_2^2) + 12x_1x_2 - 1 - t$ and $a(x) = x_1 + x_2$. Initially, at $t = 0$, the scalar field function $u(x_1, x_2, t)$ has the form

$$u(x_1, x_2, 0) = x_1^3 + x_2^3.$$

The following time-dependent mixed boundary conditions are applied on the square domain:

$$u(x_1, 1, t) = x_1^3 + 1 + t, \qquad u(x_1, 2, t) = x_1^3 + 8 + t,$$
$$\frac{\partial u(1, x_2, t)}{\partial n} = -3(1 + x_2), \qquad \frac{\partial u(2, x_2, t)}{\partial n} = 12(2 + x_2).$$

The exact solution of this problem is $u(x_1, x_2, t) = x_1^3 + x_2^3 + t$. Test 5 has variable material parameter $a(x)$ and variable time-dependent $D(x, t)$. Fig. 7 plots the RMS error for the final time step for RIBIE, RIBIDE and SDBDIE. It can be clearly seen that superior accuracy and convergence are obtained with mesh refinement. As for tests 1–4, the SDBDIE provides greater accuracy than the RIBIE and RIBIDE.

8. Conclusion

In this paper, the BDIE and BDIDE formulations are derived for the two-dimensional diffusion equation with variable coefficients. The RIM is used to transform the domain integrals appearing in both the BDIE and BDIDE formulations. Furthermore, we propose the SDBDIE approach which results in a sparse system of equations, thus avoiding the need to calculate a large number of domain integrals. The discretization used in this paper leads to an overdetermined system of linear equations.

The resulting RIBIE, RIBIDE and SDBDIE formulations are developed and implemented for the numerical solution of three possible cases: homogeneous, non-homogeneous and variable coefficient diffusion equations. From the numerical results presented in this paper, we can conclude that the SDBDIE yields the lowest errors in comparison to the RIBIE and RIBIDE but this may be due to the use of interpolation and time marching schemes of higher order.

Using the RIM, it is possible to transform the domain integrals that appear in both BDIE and BDIDE methods into equivalent boundary integrals, thus retaining the boundary-only character of the standard BEM, while the SDBDIE requires domain integration. Moreover, the RIM removes the weak singularities appearing in the domain integrals.

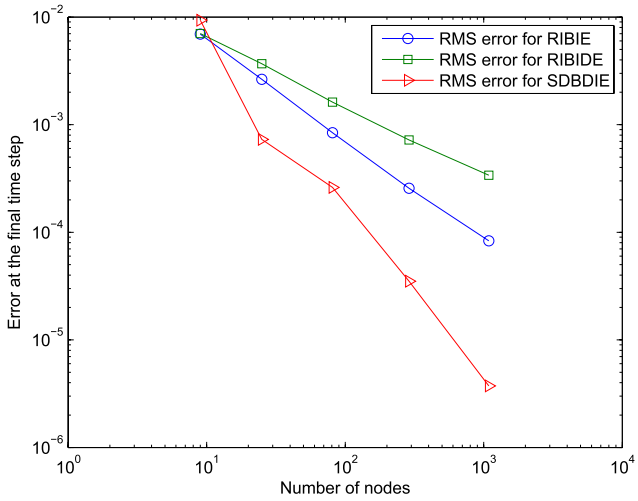

Fig. 7. RMS error for RIBIE, RIBIDE and SDBDIE methods for test 5 with $\Delta t = 0.1$.

References

[1] W.T. Ang, A Beginners Course in Boundary Element Methods, Universal Publishers, Boca Raton, FL, 2007.
[2] L.C. Wrobel, The Boundary Element Method, Vol. 1, Wiley, Chichester, 2002.
[3] C.A. Brebbia, J.C.F. Telles, L.C. Wrobel, Boundary Element Techniques, Springer, Berlin, 1984.
[4] F. Paris, J. Canas, Boundary Element Method Fundamentals and Applications, Oxford University Press, New York, 1997.
[5] D.L. Clements, Fundamental solutions for second order linear elliptic partial differential equations, Comp. Mech. 22 (1998) 26–31.
[6] W.T. Ang, J. Kusuma, D.L. Clements, A boundary element method for a second order elliptic partial differential equation with variable coefficients, Eng. Anal. Bound. Elem. 18 (1996) 311–316.
[7] R.P. Shaw, Green's functions for heterogeneous media potential problems, Eng. Anal. Bound. Elem. 13 (1994) 219–221.
[8] R.P. Shaw, G.S. Gipson, A BIE formulation of a linearly layered potential problem, Eng. Anal. Bound. Elem. 16 (1995) 1–3.
[9] A.J. Kassab, E. Divo, A generalized boundary integral equation for isotropic heat conduction with spatially varying thermal conductivity, Eng. Anal. Bound. Elem. 18 (1996) 273–286.
[10] H. Power, On the existence of Kassab and Divo's generalized boundary integral equation formulation for isotropic heterogeneous steady state heat conduction problems, Eng. Anal. Bound. Elem. 20 (1997) 341–345.
[11] M. Bonnet, M. Guiggiani, Comments about the paper entitled "A generalized boundary integral equation for isotropic heat conduction with spatially varying thermal conductivity" A.J. Kassab, E. Divo, Eng. Anal. Bound. Elem. 22 (1998) 235–240.
[12] D. Nardini, C.A. Brebbia, A new approach for free vibration analysis using boundary elements, in: C.A Brebbia (Ed.), Boundary Element Methods in Engineering, Springer, Berlin, 1982, pp. 312–326.
[13] P.W. Partridge, C.A. Brebbia, L.C. Wrobel, The Dual Reciprocity Boundary Element Method, Computational Mechanics Publication, Southampton, 1992.
[14] X.W. Gao, The radial integration method for evaluation of domain integrals with boundary-only discretization, Eng. Anal. Bound. Elem. 26 (2002) 905–916.
[15] X.W. Gao, A boundary element method without internal cells for two-dimensional and three-dimensional elastoplastic problems, ASME J. Appl. Mech. 69 (2002) 154–160.
[16] X.W. Gao, Boundary element analysis in thermoelasticity with and without internal cells, Internat. J. Numer. Methods Engrg. 57 (2003) 975–990.
[17] X.W. Gao, A meshless BEM for isotropic heat conduction problems with heat generation and spatially varying conductivity, Internat. J. Numer. Methods Engrg. 66 (2006) 1411–1431.
[18] E.L. Albuquerque, P. Sollero, W.P. Paiva, The radial integration method applied to dynamic problems of anisotropic plates, Comm. Num. Methods Eng. 23 (2007) 805–818.
[19] X.W. Gao, C.H. Zhang, L. Guo, Boundary-only element solutions of 2D and 3D nonlinear and nonhomogeneous elastic problems, Eng. Anal. Bound. Elem. 31 (2007) 974–982.
[20] W.S. Venturini, Further developments of boundary element formulation for zoned domain problems, in: C.A Brebbia, J.J. Connor (Eds.), Advances in Boundary Elements, Computational Mechanics Publications, Southampton and Springer-Verlag, Berlin, New York, 1989, pp. 251–267.
[21] I. Brunton, Solving variable coefficient partial differential equations using the boundary element method, PhD Thesis, University of Auckland, New Zealand, 1996.
[22] M.A. AL-Jawary, L.C. Wrobel, Numerical solution of two-dimensional mixed problems with variable coefficients by the boundary–domain integral and integro-differential equation methods, Eng. Anal. Bound. Elem. 35 (2011) 1279–1287.
[23] M.A. AL-Jawary, L.C. Wrobel, Numerical solution of the two-dimensional Helmholtz equation with variable coefficients by the radial integration boundary integral and integro-differential equation methods, Int. J. Comput. Math. 89 (2012) 1463–1487.
[24] M.A. AL-Jawary, L.C. Wrobel, Radial integration boundary integral and integro-differential equation methods for two-dimensional heat conduction problems with variable coefficients, Eng. Anal. Bound. Elem. 36 (2012) 685–695.
[25] S.E. Mikhailov, Localized boundary–domain integral formulations for problems with variable coefficients, Eng. Anal. Bound. Elem. 26 (2002) 681–690.
[26] S.E. Mikhailov, I.S. Nakhova, Mesh-based numerical implementation of the localized boundary–domain integral equation method to a variable-coefficient Neumann problem, J. Eng. Math. 51 (2005) 251–259.
[27] E.A. Divo, A.J. Kassab, Transient non-linear heat conduction solution by a dual reciprocity boundary element method with an effective a posteriori error estimator, Comp. Mat. Cont. 2 (2005) 277–288.
[28] L.C. Wrobel, C.A. Brebbia, D. Nardini, The dual reciprocity boundary element formulation for transient heat conduction, in: A. Sa da Costa, A. Melo Baptiste, W.G. Gray, C.A. Brebbia, G.F. Pinder (Eds.), Finite Elements in Water Resources VI, Springer, Berlin, 1986.
[29] L.C. Wrobel, C.A. Brebbia, The dual reciprocity boundary element formulation for nonlinear diffusion problems, Comp. Methods Appl. Mech. Engrg. 65 (1987) 147–164.
[30] M.R. Hematiyan, G. Karami, A meshless boundary element method formulation for transient heat conduction problems with heat sources, Scientia Iranica 15 (2008) 348–359.
[31] K. Yang, X.W. Gao, Radial integration BEM for transient heat conduction problems, Eng. Anal. Bound. Elem. 34 (2010) 557–563.

[32] K. Yang, X.W. Gao, Y.F. Liu, Using analytical expressions in radial integration BEM for variable coefficient heat conduction problems, Eng. Anal. Bound. Elem. 35 (2011) 1085–1089.
[33] V.L. Greengard, Rokhlin, A new version of the fast multipole method for the Laplace equation in three dimensions, Acta Numer. 6 (1997) 229–269.
[34] J. Ravnik, L. Škerget, M. Hriberšek, The wavelet transform for BEM computational fluid dynamics, Eng. Anal. Bound. Elem. 28 (2004) 1303–1314.
[35] V. Popov, H. Power, L. Škerget, Domain Decomposition Techniques for Boundary Elements Application to Fluid Flow, WIT Press, Southampton, Boston, MA, 2007.
[36] M. Bebendorf, Approximation of boundary element matrices, Numer. Math. 86 (2000) 565–589.
[37] S. Börm, L. Grasedyck, W. Hackbusch, Introduction to hierarchical matrices with applications, Eng. Anal. Bound. Elem. 27 (2003) 405–422.
[38] J. Ravnik, L. Škerget, Z. Žunič, Velocity–vorticity formulation for 3D natural convection in an inclined enclosure by BEM, Int. J. Heat Mass Transfer 51 (2008) 4517–4527.
[39] J. Ravnik, L. Škerget, Z. Žunič, Comparison between wavelet and fast multipole data sparse approximations for Poisson and kinematics boundary–domain integral equations, Comput. Methods Appl. Mech. Eng. 198 (2009) 1473–1485.
[40] M. Ramšak, L. Škerget, A subdomain boundary element method for high-Reynolds laminar flow using stream function–vorticity formulation, Internat. J. Numer. Methods Fluids 46 (2004) 815–847.
[41] J. Ravnik, L. Škerget, Z. Žunič, Combined single domain and subdomain BEM for 3D laminar viscous flow, Eng. Anal. Bound. Elem. 33 (2009) 420–424.
[42] M.A. AL-Jawary, L.C. Wrobel, Numerical solution of a mixed problem with variable coefficients by the boundary–domain integral and integro-differential equation methods, in: IABEM 2011, University of Brescia Press, Brescia, Italy, 2011, pp. 19–26.
[43] S.N. Fata, Treatment of domain integrals in boundary element methods, Appl. Numer. Math. 62 (2012) 720–735.
[44] T.R. Bridges, L.C. Wrobel, A dual reciprocity formulation for elasticity problems with body forces using augmented thin plate splines, Comm. Num. Meth. Eng. 12 (1996) 209–220.
[45] S.R. Karur, P.A. Ramachandran, Augmented thin plate spline approximation in DRM, Boun. Elem. Comm. 6 (1995) 55–58.
[46] Leilei Cao, Qing-Hua Qin, Ning Zhao, Application of DRM-Trefftz and DRM-MFS to transient heat conduction analysis, Recent Patents Space Technol. 2 (2010) 41–50.
[47] W. Hoitinga, Direct minimization of equation residuals in least squares hp-finite element methods: a direct and iterative solution method, Internal Report, Delft University of Technology, The Netherlands, 2004.
[48] P.B. Hansen, Householder reduction of linear equations, Assoc. Comput. Mach. 24 (1992) 185–194.
[49] W. Hoitinga, R. de Groot, M. Kwakkel, M. Gerritsma, Direct minimization of the least-squares spectral element functional - part I: direct solver, J. Comput. Phys. 227 (2008) 2411–2429.
[50] http://www.mathworks.co.uk/help/toolbox/stats/regress.html.
[51] S. Chatterjee, A.S. Hadi, Influential observations, high leverage points, and outliers in linear regression, Statist. Sci. 1 (1986) 379–416.